

High-mobility group box protein 1 promotes the survival of myeloid-derived suppressor cells by inducing autophagy

Katherine H. Parker, Lucas A. Horn, and Suzanne Ostrand-Rosenberg¹

Department of Biological Sciences, University of Maryland Baltimore County, Baltimore, Maryland, USA

RECEIVED JULY 16, 2015; REVISED JANUARY 4, 2016; ACCEPTED JANUARY 18, 2016. DOI: 10.1189/jlb.3HI0715-305R

ABSTRACT

Myeloid-derived suppressor cells are immune-suppressive cells that are elevated in most individuals with cancer, where their accumulation and suppressive activity are driven by inflammation. As myeloid-derived suppressor cells inhibit anti-tumor immunity and promote tumor progression, we are determining how their viability is regulated. Previous studies have established that the damage-associated molecular pattern molecule high-mobility group box protein 1 drives myeloid-derived suppressor cell accumulation and suppressive potency and is ubiquitously present in the tumor microenvironment. As high-mobility group box protein 1 also facilitates tumor cell survival by inducing autophagy, we sought to determine if high-mobility group box protein 1 regulates myeloid-derived suppressor cell survival through induction of autophagy. Inhibition of autophagy increased the quantity of apoptotic myeloid-derived suppressor cells, demonstrating that autophagy extends the survival and increases the viability of myeloid-derived suppressor cells. Inhibition of high-mobility group box protein 1 similarly increased the level of apoptotic myeloid-derived suppressor cells and reduced myeloid-derived suppressor cell autophagy, demonstrating that in addition to inducing the accumulation of myeloid-derived suppressor cells, high-mobility group box protein 1 sustains myeloid-derived suppressor cell viability. Circulating myeloid-derived suppressor cells have a default autophagic phenotype, and tumor-infiltrating myeloid-derived suppressor cells are more autophagic, consistent with the concept that inflammatory and hypoxic conditions within the microenvironment of solid tumors contribute to tumor progression by enhancing immune-suppressive myeloid-derived suppressor cells. Overall, these results demonstrate that in addition to previously

recognized protumor effects, high-mobility group box protein 1 contributes to tumor progression by increasing myeloid-derived suppressor cell viability by driving them into a proautophagic state. *J. Leukoc. Biol.* 100: 463–470; 2016.

Introduction

Solid tumors often generate a harsh local environment containing multiple proinflammatory mediators [1]. Tumor progression requires that tumor cells, as well as immune-suppressive host cells, must survive in this TME. Survival of malignant cells is, at least partially, a result of autophagy. Many tumor cells are autophagic, even under minimally stressful conditions, whereas nonmalignant cells usually become autophagic only in response to stress [2]. Autophagy is triggered by a variety of conditions present in the TME, including nutrient deprivation and hypoxia. It provides a survival advantage to stressed cells, as it enables cells to maintain metabolic activity by engulfing cytoplasmic components that are degraded in autolysosomes [3]. Degradation of cytoplasmic components through starvation-induced autophagy regenerates amino acids that are used in the tricarboxylic acid cycle to produce energy that the cell needs to survive, thus allowing them to avoid death [4].

Autophagy involves the formation of autophagosomes, mediated by a series of membrane rearrangements involving Atg protein [5] (Fig. 1). Autophagy is initiated when mTOR is down-regulated, resulting in the release of the transcription factor Unc-51-like autophagy-activating kinase 1, which in turn, induces vacuole formation by activating PI3KC3, Beclin1 (Atg6), and the Atg12, -5, and -16 complex. This complex then interacts with Atg9 to mediate the induction of an autophagosome [6]. Once an autophagosome is formed, Atg4, -7, and -3 assist in modifying LC3 (Atg8), first into LC3-I through cleavage by a cysteine protease and further into LC3-II by conjugation with a phosphatidylethanolamine. LC3-II is then incorporated into the lumen of an autophagosome. Upon closure of the autophagosome, adaptor proteins, such as p62, are retained

Abbreviations: APC = allophycocyanin, Atg = autophagy-related gene, CHOP = C/EBP homologous protein, DAMP = damage-associated molecular pattern molecule, EBSS = Earl's balanced salt solution, FasL = Fas ligand, HA = hemagglutinin, HL-1 = serum-free media, HMGB1 = high-mobility group box protein 1, IRF8 = IFN regulatory factor 8, LC3 = microtubule-associated protein 1 light chain 3, MCF = mean channel

(continued on next page)

The online version of this paper, found at www.jleukbio.org, includes supplemental information.

1. Correspondence: Dept. of Biological Sciences, University of Maryland Baltimore County, 1000 Hilltop Circle, Baltimore, MD 21250, USA. E-mail: srosenbe@umbc.edu

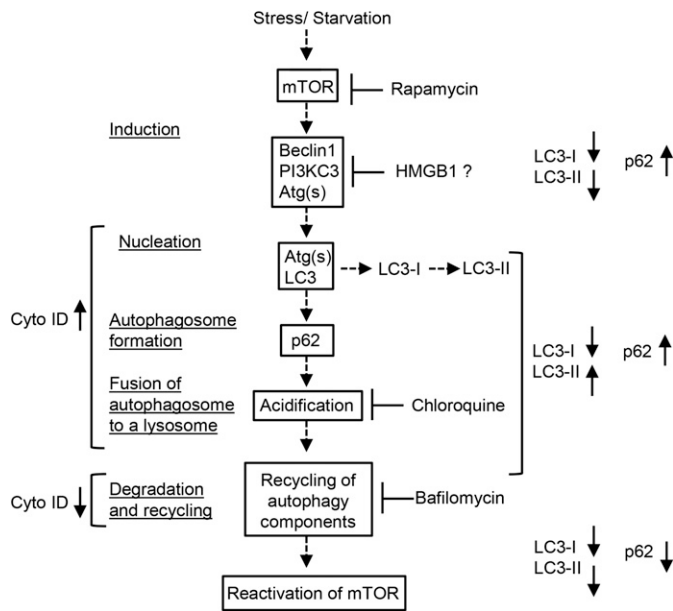


Figure 1. Autophagic flux. Autophagy is initiated by inhibition of mTOR, which is caused by stress, starvation, or treatment with rapamycin. Following inactivation of mTOR, Beclin1, PI3KC3, and Atg, proteins are activated, and nucleation occurs with the assistance of additional Atg proteins. LC3 is then modified to give rise to LC3-I, which generates LC3-II and aids in forming the double-membrane autophagosome. The autophagosome contains adaptor proteins, such as p62, which aid in targeting cargo proteins. An autophagosome will mature into an autolysosome following fusion with a lysosome, creating an acidic internal environment. The acidic environment of the autolysosome allows for degradation and recycling of autophagosome components, eventually leading to the reactivation of mTOR once stress/starvation are resolved. Autophagic flux can be monitored in live cells using a Cyto-ID stain (left) or by Western blot analysis of LC3 and p62 (right). Chloroquine and bafilomycin block autophagy at the acidification and recycling stages, respectively. ↓, Molecules that are down-regulated; ↑, molecules that are up-regulated; dotted down arrow, the direction of events in autophagy.

within the autophagosome and target cargo for degradation. An autophagosome will mature into an autolysosome by docking and fusing with a lysosome. The autolysosome allows for the breakdown and recycling of autophagosomal contents, which temporarily sustain survival.

Immune-suppressive cells in the TME are important contributors to tumor progression, as they prevent the host's immune system from eliminating malignant cells [7]. MDSCs are a major population of such suppressive cells and are present in the TME of most individuals with solid tumors [8]. A study by Ostrand-Rosenberg and Sinha [9] has established that multiple proinflammatory mediators induce the accumulation and suppressive potency of MDSCs. The DAMP protein HMGB1 is ubiquitously present in the TME, is an established driver of MDSC development

(continued from previous page)

fluorescence, MDSC = myeloid-derived suppressor cell, mTOR = mechanistic target of rapamycin, p62 = phosphotyrosine-independent ligand for the Lck Src homology 2 domain p62, PI = propidium iodide, PI3KC3 = PI3K, catalytic subunit 3, ROS = reactive oxygen species, TME = tumor microenvironment

and function [10], and is also an inducer of tumor cell autophagy [11]. These properties of HMGB1 raise the question of whether MDSC survival in the TME is prolonged as a result of autophagy.

With the use of inhibitors and inducers of autophagy and inhibitors of HMGB1, we have assessed the role of HMGB1 and autophagy in the survival of tumor-induced MDSC. Our results indicate that in addition to promoting MDSC development, HMGB1 prolongs MDSC survival by driving MDSC autophagy, and that the TME promotes autophagy in MDSCs.

MATERIALS AND METHODS

Mice

BALB/c, BALB/c DO11.10 (TCR transgenic for the $\alpha\beta$ -TCR specific for OVA peptides 323–339 restricted by I-A^d), and BALB/c clone 4 TCR-transgenic ($\alpha\beta$ -TCR specific for influenza HA 518–526 restricted by H-2K^d) mice were purchased from The Jackson Laboratory (Bar Harbor, ME, USA) and/or bred in the University of Maryland Baltimore County (UMBC) Biology Department Animal Facility (Baltimore, MD, USA). Female mice, <6 mo of age, were used for all experiments. All animal procedures were approved by the UMBC Institutional Animal Care and Use Committee.

Reagents, antibodies, and cells

Heparin sodium salt (grade IA), chloroquine, hyaluronidase, deoxyribonuclease I, and ethyl pyruvate were purchased from Sigma-Aldrich (St. Louis, MO, USA). Bafilomycin and rapamycin were purchased from Cayman Chemical (Ann Arbor, MI, USA). Collagenase type 4 was purchased from Worthington Biochemical (Lakewood, NJ, USA). Ficol-Paque PLUS was purchased from GE Healthcare Life Sciences (Pittsburgh, PA, USA). Fluorescently coupled antibodies Gr1-APC (RB6-8C5), CD8-APC (53-6.7), CD4-PE (GK1.5), V β 8.1 8.2-PE (MR5-2), Annexin V-FITC, PI, and Annexin V binding buffer were from BD Biosciences (San Jose, CA, USA). CD11b-Pacific Blue (M1/70) and CD45-APC-Cy7 (30-F11) were from BioLegend (San Diego, CA, USA). DO11.10-APC (KJ1-26) was from eBioscience (San Diego, CA, USA). Murine 4T1 and human Jurkat cells were cultured in IMDM, supplemented with 10% fetal bovine product, 1% penicillin, 1% streptomycin, 1% glutamax, and 1% gentamycin. HeLa cells were cultured in DMEM, supplemented with 10% FCS, 1% penicillin, 1% streptomycin, 1% glutamax, and 1% gentamycin.

Tumor inoculations

BALB/c mice were inoculated in the abdominal mammary fat pad, with 7×10^3 4T1 mammary carcinoma cells. 4T1 cells have been in the authors' laboratory for >20 y. They were originally obtained from Dr. Fred Miller at the Karmanos Cancer Center (Detroit, MI, USA).

Flow cytometry

Cells were labeled for immunofluorescence and analyzed by flow cytometry for cell-surface molecules by staining with antibodies to Gr1 and CD11b. Antibodies were diluted in PBS containing 2% FCS (HyClone). Staining was conducted in the dark, on ice for 30 min. Staining for apoptosis or autophagy was conducted after surface staining. For apoptosis staining, 1×10^6 cells were stained with PI and Annexin V for 15 min at room temperature, per the manufacturer's protocol (BD Biosciences). For Cyto-ID staining, cells were first stained for surface markers, Gr1 and CD11b, followed by staining with Cyto-ID for 30 min at 37°C, per the manufacturer's protocol (Enzo Life Sciences, Farmingdale, NY, USA). Samples were run on a Cyan ADP flow cytometer and analyzed using Summit 4.3 software (Beckman Coulter, Brea, CA, USA).

MDSCs

BALB/c mice with large 4T1 tumors (9–12 mm in diameter) were bled from the submandibular vein into 1 ml PBS containing 0.008% heparin. RBCs were

removed by Gey's treatment, as described [12]. The remaining leukocytes were stained for Gr1 and CD11b and analyzed by flow cytometry. Populations that were >90% Gr1⁺CD11b⁺ were used in experiments.

Isolation of tumor-infiltrating cells from solid tumors

Tumors were dissociated using a modified protocol from the Tissue Dissociation Kit (Protocol 2.2.1; Miltenyi Biotec, Auburn, CA, USA). Tumors (9–12 mm diameter) were excised from BALB/c mice and minced with scissors into small pieces inside of gentleMACS C Tubes containing DMEM media, supplemented with 2000 U/ml DNase, 300 U/ml collagenase, and 0.1% hyaluronidase. Tumor chunks were then dissociated into single-cell suspensions using a gentleMACS Dissociator (program m_impmtumor_02; Miltenyi Biotec), followed by rotation (10 rpm; Glas-Col Rotator, Terre Haute, IN, USA) at 37°C for 40 min and a second round of dissociation and rotation. Resulting cells were passed through 70 µm filters, rinsed twice with PBS, resuspended in IMDM, and then centrifuged on a Ficoll-Paque PLUS gradient at 1230 *g* (Eppendorf centrifuge 5810R; 20°C for 20 min). Tumor-infiltrating cells were harvested from the interphase of the gradient and then rinsed twice with PBS.

Starvation-induced autophagy

To induce autophagy, cells were cultured in HBSS for 3 h or in EBSS for 4 h at 37°C in a 5% CO₂/95% air incubator. Nonstarved control cell lines were maintained in their culture media under the same conditions as starved cells. Nonstarved control MDSCs were cultured in their growth medium (HL-1) without additional supplements.

MDSC viability

MDSC survival was assessed according to the procedure of Tang et al. [13]. In brief, MDSCs from 4T1 tumor-bearing BALB/c mice were harvested and incubated in HL-1, with or without ethyl pyruvate (20 mM) or diluent control (PBS) at 37°C in a 5% CO₂/95% air incubator. After 1 h, MDSCs were transferred to HBSS, returned to the incubator, and starved for 3 h, with or without ethyl pyruvate (20 mM) or diluent control. In some experiments,

MDSCs were incubated overnight in growth medium or for 4 h in EBSS with the autophagy inducer rapamycin (1 µM), autophagy inhibitor chloroquine (5 µM) or bafilomycin (0.1 µM), or the respective diluent controls (water for chloroquine or DMSO for rapamycin and bafilomycin). Data were normalized so that the untreated sample (no drug) represented 100% viability, as calculated by no-drug MCF/100 = *x*; all data were then multiplied by *x*. Percent MDSC viability = [(experimental % viable) – (diluent control % viable – untreated % viable)].

Autophagy activity

4T1-induced MDSC, 4T1, Jurkat, and HeLa cells were starved for 4 h in EBSS in the presence of ethyl pyruvate (20 mM) or bafilomycin (0.1 µM) or their respective diluent controls (PBS for ethyl pyruvate; DMSO for bafilomycin). After starvation, autophagic vacuoles were detected by staining with Cyto-ID, per the manufacturer's protocol (Enzo Life Sciences). Data were normalized so that autophagy activity (MCF) following starvation (EBSS only) = 100%. Percent autophagy activity = [(experimental_{MCF}) – (diluent control_{MCF} – untreated_{MCF})] / (experimental_{MCF}) / (tumor-free_{MCF}).

T cell activation

MDSCs were isolated from 4T1 tumor-bearing BALB/c mice and starved in EBSS in the presence of rapamycin (1 µM), chloroquine (5 µM), bafilomycin (0.1 µM), or the respective diluent control (water for chloroquine; DMSO for rapamycin and bafilomycin) and used immediately in T cell activation assays, as described previously [12]. In brief, splenocytes from TCR-transgenic mice (1 × 10⁵ cells) and irradiated (25 Gy) MDSCs (2, 1, 0.5, or 0.25 × 10⁵ cells) were cocultured in flat-bottom, 96-well plates in 200 µl HL-1 media containing 1% penicillin, 1% streptomycin, 1% glutamax, and 5 × 10⁻³ M 2-ME/well. OVA_{323–339} (14 µM) or HA_{518–526} (28 µM) peptide was included for DO11.10 and clone 4 cells, respectively. On d 3, 1 µCi [³H]-thymidine in 50 µl medium was added to each well. Eighteen hours later, the cells were harvested, and [³H]-thymidine incorporation was measured by scintillation counter. Data are expressed as cpm ± SD of triplicate cultures.

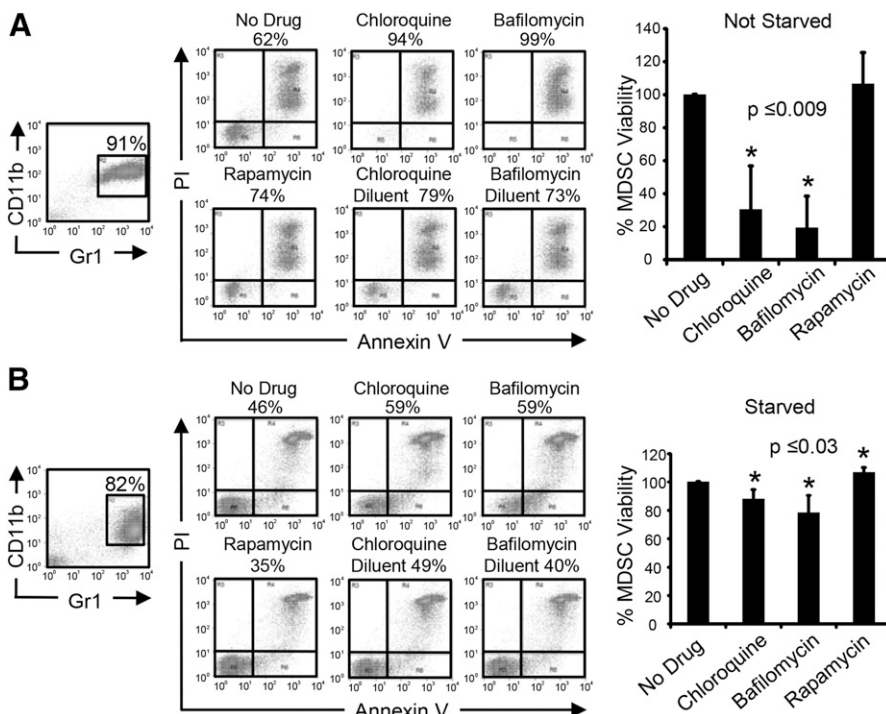


Figure 2. Autophagy promotes MDSC survival. (A) MDSCs were obtained from the blood of 4T1 tumor-bearing BALB/c mice and assessed for purity by flow cytometry analysis of Gr1 and CD11b expression (left). MDSCs were incubated overnight under nonstarvation conditions (HL-1 medium) in the presence or absence of autophagy inhibitors chloroquine (5 µM) or bafilomycin (0.1 µM), autophagy-inducer rapamycin (1 µM), or the respective diluent controls. After incubation, MDSCs were stained for Gr1, CD11b, Annexin V, and PI and the gated Gr1⁺CD11b⁺ cells analyzed for Annexin V and PI. Dot plots (left) show percent dead (AnnexinV⁺PI⁺) MDSCs for a representative mouse. The graph (right) shows the average percent viable MDSCs for 3 mice (**P* < 0.009). (B) MDSCs were obtained and treated as in A, except cells were incubated for 4 h under starvation conditions (EBSS medium). **P* < 0.03, statistical significant difference compared with nontreated samples. Data were normalized so that the no-drug control groups were 100% viable. Flow profiles are from 1 of 3 independent experiments. Graphs are averaged from 3 independent experiments.

Western blots

Jurkat, HeLa, and 4T1 cells were harvested when 75% confluent. After harvesting, 1×10^7 cells were starved in 25 ml EBBS for 4 h in the presence of ethyl pyruvate (10 mM), rapamycin (1 μ M), chloroquine (500 μ M for 4T1 and 10 μ M for HeLa and Jurkat), bafilomycin (0.1 μ M), or the respective diluent controls (PBS for ethyl pyruvate, DMSO for rapamycin and bafilomycin, water for chloroquine). After starvation, cells were rinsed with PBS and then lysed in 300 μ l M-PER mammalian protein extraction reagent (Thermo Fisher Scientific, Grand Island, NY, USA). Whole-cell lysate (50 μ g) was then mixed with 6 \times sample buffer (0.375 mM Tris HCl, 9% SDS, 50% glycerol, 0.03% bromophenol blue, and 9% 2-ME), heated for 5 min at 95°C, and electrophoresed on 14% SDS-PAGE gels [SDS running buffer (Bio-Rad Laboratories, Hercules, CA, USA), 150 V, 1 h]. Proteins were transferred to polyvinylidene difluoride membranes (GE Healthcare Life Sciences) using a Mini Trans-blot cell (30 V; transfer buffer, overnight; Bio-Rad Laboratories). Membranes were blocked with 5% nonfat dried milk or 0.2% I-Block (Applied Biosystems, Thermo Fisher Scientific) in TBST. LC3 was detected with anti-LC3B antibody (Novus Biologicals, Littleton, CO, USA; 1.4 μ g/ml in 7 ml 1% BSA/5% milk/TBST), followed by goat anti-rabbit secondary antibody (EMD Millipore, Billerica, MA, USA; 40 ng/ml in 10 ml 1% BSA/5% milk/TBST). p62 was detected with anti-p62 antibody (Novus Biologicals; 22.8 ng/ml in 10 ml 0.2% I-Block/TBST), followed by goat anti-rabbit secondary antibody (40 ng/ml in 10 ml 5% milk/TBST). β -Actin was detected with anti- β -actin antibody (Sigma-Aldrich; 50 ng/ml in 10 ml 2.5% milk/TBST), followed by sheep anti-mouse secondary antibody (EMD Millipore; 40 ng/ml in 10 ml 2.5% milk/TBST). Bands were visualized using an HRP detection kit on X-ray film (both from Denville Scientific, Holliston, MA, USA).

Statistical analysis

Student's *t* test was used to determine statistical significance between 2 sets of data. Single-factor ANOVA was used to determine significance between groups of data. Significance levels are indicated in figure legends by an *.

RESULTS

Autophagy promotes MDSC survival

If MDSC survival is facilitated by autophagy, then the inhibition of autophagy will reduce the viability of MDSCs. To test this hypothesis, the autophagy inhibitors chloroquine and bafilomycin and the autophagy inducer rapamycin were used. To assure that results could be ascribed to autophagy and not to nonspecific killing, circulating MDSCs from BALB/c mice with large 4T1 tumors were cultured under starvation conditions for 4 h with titrated amounts of each drug to identify a dose that was not toxic (Supplemental Fig. 2). Nontoxic doses were identified, then 4T1-induced MDSCs were cultured overnight in HL-1 medium in the presence of the drugs, and MDSC viability was assessed by staining cells for CD11b, Gr1, PI, and Annexin V (Fig. 2A). Treatment with chloroquine or bafilomycin reduced MDSC viability by 70% and 81%, respectively, relative to their diluent controls, whereas rapamycin did not significantly alter MDSC viability. [Dot plots show percent dead (AnnexinV⁺PI⁺) MDSCs from a representative mouse; the graph shows the average percent viability of MDSC from 3 mice.]

These results establish that under nonstressed conditions, MDSCs use autophagy to enhance viability, and the default condition of tumor-induced MDSCs is as proautophagic cells.

To assess if MDSCs in starved settings use autophagy to survive, MDSCs were starved for 4 h in serum-free EBSS medium to induce autophagy and then stained for CD11b, Gr1, PI, and

Annexin V (Fig. 2B). The autophagy inhibitors chloroquine and bafilomycin reduced the viability of CD11b⁺Gr1⁺ MDSC by 12% and 22%, respectively, whereas the autophagy inducer rapamycin increased MDSC viability by 7%. [Dot plots show percent dead (AnnexinV⁺PI⁺) MDSCs; the graph shows percent viable MDSC.] These results demonstrate that MDSCs use autophagy to survive in starvation conditions.

HMGB1 promotes MDSC survival

Our previous studies established that HMGB1 is ubiquitously present in the TME and drives the accumulation of MDSCs from bone marrow progenitor cells and the immune-suppressive potency of MDSCs, thereby identifying HMGB1 as a proinflammatory mediator in MDSC development and function [10]. Studies by others demonstrated that HMGB1 facilitates the survival of tumor cells by converting them to an autophagic state [13]. These findings led us to hypothesize that HMGB1 may sustain MDSC viability by promoting MDSC autophagy. If HMGB1 promotes MDSC autophagy, then inhibition of HMGB1 during conditions that drive MDSC autophagy will reduce MDSC viability. As HMGB1 is constitutively released by MDSCs [10, 14], we assessed this possibility by culturing MDSCs under starvation conditions in the presence or absence of the

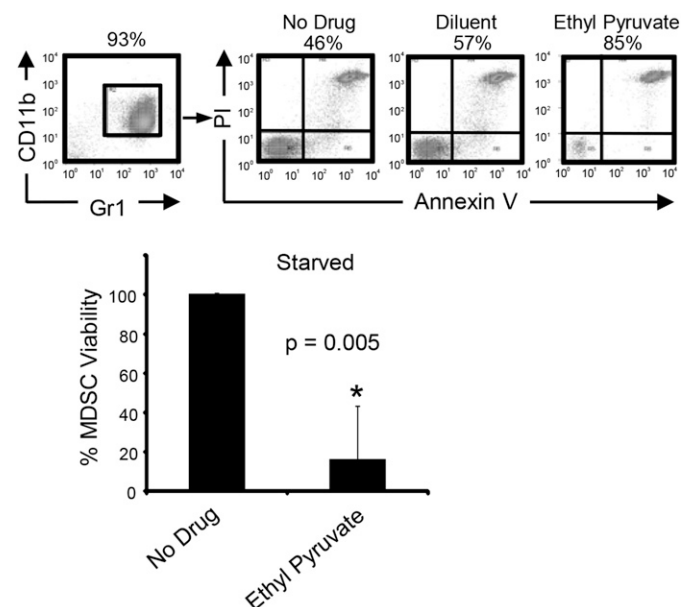


Figure 3. HMGB1 promotes MDSC survival. MDSCs were obtained from the blood of 4T1 tumor-bearing BALB/c mice, and an aliquot was assessed for purity by flow cytometry analysis of Gr1 and CD11b expression (upper left histogram). MDSCs were incubated for 1 h in HL-1 medium in the presence or absence of the HMGB1 inhibitor ethyl pyruvate (20 mM) or diluent control (PBS) and subsequently starved in HBSS for 3 h, with or without ethyl pyruvate or diluent control. After incubation, MDSCs were stained and analyzed as in Fig. 2. PI and Annexin V staining of MDSCs from a representative individual mouse (upper histogram); average percent MDSC viability for 3 mice (lower). **P* = 0.005, statistical significant difference compared with starved samples. Data were normalized so that the no-treatment control group was 100% viability. Flow profiles are from 1 of 3 independent experiments. The graph is averaged from 3 independent experiments.

HMGB1 inhibitor ethyl pyruvate, which blocks the release of HMGB1 [14] (Fig. 3). Ethyl pyruvate was used at a dose that is not toxic to MDSCs [10], and MDSCs subjected to starvation-induced autophagy in the presence of ethyl pyruvate were 84% less viable than control-treated cells, demonstrating that HMGB1 enhances the survival of autophagic MDSCs.

HMGB1 promotes autophagy in MDSC

To assess if HMGB1 enhances MDSC survival by inducing autophagy, MDSC autophagic flux was assessed by flow cytometry using the fluorescent dye Cyto-ID that stains autophagic vacuoles (see Fig. 1). The dye is a cationic amphiphilic tracer that partitions into cells and stains preautophagosomes and autophagosomes. It interacts with hydrophobic lamellar structures of autophagic vacuoles and therefore, colocalizes with LC3, which is an essential marker for autophagosomes [15, 16]. Bafilomycin-induced inhibition of autophagy reduces Cyto-ID staining and thus, serves as a control [17].

If HMGB1 promotes autophagy in MDSCs, then inhibition of HMGB1 under conditions that drive autophagy will decrease autophagy activity. To test this possibility, MDSCs were cultured under starvation conditions in the presence or absence of the autophagy inhibitor bafilomycin or HMGB1 inhibitor ethyl pyruvate and subsequently stained with Cyto-ID and analyzed by flow cytometry. Treatment with the autophagy inhibitor bafilomycin served as a control (Fig. 4A). Autophagy activity of MDSC was reduced 53% when ethyl pyruvate was included in the cultures. A 65% reduction in autophagy activity was observed

when bafilomycin was included instead of ethyl pyruvate. Therefore, inhibition of HMGB1 and treatment with bafilomycin similarly reduce the level of autophagy in MDSCs, demonstrating that HMGB1 regulates autophagic flux in MDSC.

Western blotting for the autophagy markers LC3 and p62 is conventionally used to assess autophagy. We have used Cyto-ID and flow cytometry for the MDSC studies, as Cyto-ID staining is more sensitive, and MDSC material is limiting. To confirm that Cyto-ID staining concurs with Western blotting analysis, cultured cell lines were analyzed in parallel by Cyto-ID staining and Western blotting. Jurkat cells were starved or not starved and treated with the autophagy inducer rapamycin, the autophagy inhibitors bafilomycin and chloroquine, or ethyl pyruvate and subsequently analyzed by Western blot for the autophagic markers LC3 and p62 (Fig. 4B) or by Cyto-ID and flow cytometry (Fig. 4C). As seen in the Western blots, induction of autophagy by starvation or treatment with rapamycin caused the turnover of LC3-I and the degradation of p62, indicative of increased autophagy. Inhibition of autophagy by bafilomycin or chloroquine blocked the turnover of LC3-II, causing accumulation of LC3-II, and prevented the degradation of p62, indicative of reduced autophagy. Cyto-ID staining similarly showed decreased autophagy in Jurkat cells following treatment with bafilomycin.

The Cyto-ID results with MDSC indicated that the HMGB1 inhibitor ethyl pyruvate reduced autophagy. To confirm this observation, Jurkat cells were starved or not starved in the presence or absence of ethyl pyruvate and in parallel, analyzed by Western blot (Fig. 4B) and Cyto-ID flow cytometry (Fig. 4C).

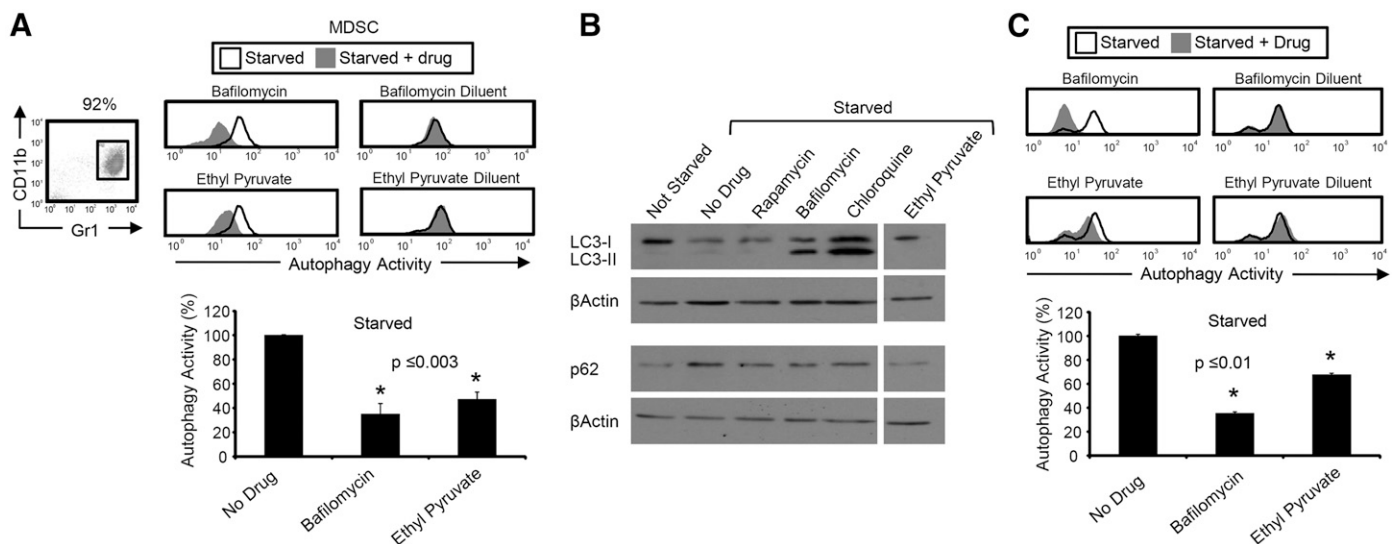


Figure 4. HMGB1 promotes autophagy in MDSC. (A) MDSCs were obtained from the blood of 4T1 tumor-bearing BALB/c mice, and an aliquot was assessed for purity by flow cytometry analysis of Gr1 and CD11b (upper left histogram). MDSCs were incubated in EBSS for 4 h in the presence of autophagy inhibitor bafilomycin (0.1 μ M), HMGB1 inhibitor ethyl pyruvate (20 mM), or the respective diluent controls. After incubation, MDSCs were stained for Gr1 and CD11b and with Cyto-ID, and the gated Gr1⁺CD11b⁺ cells were analyzed by flow cytometry for Cyto-ID expression. Cyto-ID staining for MDSC from a representative individual mouse (upper right histogram); average percent MDSC autophagy activity for 3 mice (lower graph). (B) Jurkat cells were not starved or starved and treated with rapamycin (1 μ M), bafilomycin (0.1 μ M), chloroquine (10 μ M), or ethyl pyruvate (10 mM); lysed; and assessed by Western blot for LC3, p62, and β -actin expression. (C) Jurkat cells were starved, treated, and stained as in A. Cyto-ID staining on an individual sample of Jurkat cells (upper histograms); average percent autophagy activity for 3 independent samples (lower graph). **P*, statistical significant difference compared with starved samples. Data were normalized so the starved control group is 100% autophagy activity. Data are from 1–5, 3, and 2 independent experiments for A, B, and C, respectively.

As seen in the Western blot, ethyl pyruvate reduced the accumulation of LC3-I and blocked the conversion of LC3-I into LC3-II in Jurkat cells, characteristics of autophagic flux. In contrast, p62 levels were not different in ethyl pyruvate-treated starved cells compared with untreated, not starved, cells. Cyto-ID staining similarly showed reduced autophagy in ethyl pyruvate-treated Jurkat cells, thus demonstrating the concurrence of the Western blot and Cyto-ID techniques. As p62 changes occur after LC3 degradation, the Western blot analyses provide the additional information that HMGB1 acts early to inhibit autophagy. This finding is consistent with the function of ethyl pyruvate, which is to prevent the release of HMGB1 and thereby block autophagy at its onset.

To confirm further the concurrence of Cyto-ID and Western blotting analyses, 2 additional tissue-culture cell lines were tested: murine 4T1 mammary carcinoma cells (Supplemental Fig. 1A) and human HeLa cells (Supplemental Fig. 1B) were starved or not starved; treated with rapamycin, bafilomycin, chloroquine, or ethyl pyruvate; and assayed in parallel by Western blotting and flow cytometry. 4T1 and HeLa cells gave similar results, as shown for Jurkat cells, further supporting the validity of the Cyto-ID findings for MDSC. Collectively, the Cyto-ID and Western studies demonstrate that HMGB1 promotes autophagy in Jurkat, 4T1, and HeLa cells, as well as in tumor-induced MDSCs.

Autophagy reduces MDSC-suppressive potency

Suppression of T cell activation is the hallmark function of MDSCs [8]. To determine if autophagic status affects suppressive function, MDSCs were starved and treated with the autophagy inhibitors bafilomycin or chloroquine before their incubation with antigen-specific CD4⁺ or CD8⁺ transgenic T cells and cognate peptide (Fig. 5). Bafilomycin treatment increased the suppressive activity of MDSC for CD4⁺ and CD8⁺ T cells, whereas chloroquine treatment significantly increased MDSC-suppressive activity against CD4⁺ T cells. Chloroquine-treated MDSCs also displayed a trend to be more immune suppressive. As bafilomycin and chloroquine are autophagy inhibitors, these results demonstrate that autophagy decreases the suppressive potency of MDSCs.

The TME promotes autophagy in MDSCs

To confirm the in vitro autophagy findings in the TME, cells were isolated from the blood of tumor-free and 4T1 tumor-bearing BALB/c mice and from 4T1 primary tumors of BALB/c mice and stained with antibodies to CD45, CD11b, and Gr1 and Cyto-ID. Relative autophagy activity of gated CD45⁺CD11b⁺Gr1⁺ cells was then determined using MDSCs from the blood of tumor-free mice as the reference point (Fig. 6). MDSCs from the blood of tumor-bearing mice express elevated levels of autophagy activity compared with MDSCs from tumor-free mice, whereas tumor-infiltrating MDSCs are the most autophagic. These results demonstrate that the TME enhances autophagy in MDSCs.

DISCUSSION

MDSCs are profoundly immune-suppressive cells that promote tumor progression by inhibiting anti-tumor immunity. In solid

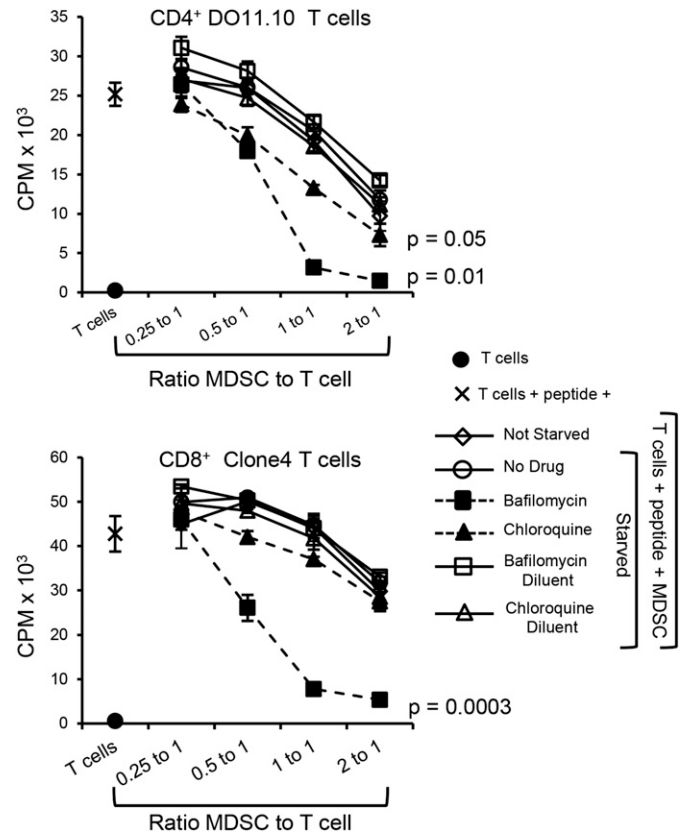


Figure 5. Autophagy decreases MDSC-mediated suppression of antigen-activated T cells. MDSCs (>87% Gr1⁺CD11b⁺) were obtained from the blood of 4T1 tumor-bearing BALB/c mice and not starved or starved in the presence of autophagy inhibitors chloroquine (5 μ M) or bafilomycin (1 μ M) or the respective diluent controls. After starvation, MDSCs were rinsed with PBS and then irradiated. Splenocytes from CD4⁺ DO11.10 (upper) or CD8⁺ clone 4 (lower) TCR-transgenic mice were cocultured with irradiated, 4T1-induced MDSC and cognate peptide (OVA or HA peptide for DO11.10 and clone 4 T cells, respectively). T cell proliferation was measured by [³H]-thymidine incorporation. Statistical significant difference compared with starved samples, as assessed by single-factor ANOVA. Data are from 1 of 2 independent experiments.

tumors, they mediate many of their effects while residing in a TME that challenges their survival as a result of less-than-optimal growth conditions. The ability of MDSCs to survive under these harsh conditions is likely a result of multiple adaptations. Here, we demonstrate that one of the adaptations invoked by tumor-induced MDSCs is to become autophagic and thereby avoid apoptosis, resulting in an increase in MDSC survival. This condition is mediated by the alarmin and DAMP, HMGB1, which is ubiquitously present in solid tumors.

Various apoptotic mechanisms have been implicated in MDSC survival. MDSCs express the death receptor Fas and can be killed by FasL-expressing activated T cells [18]. Inflammation in tumor-bearing mice increases MDSC levels [19, 20] by rendering them more resistant to Fas–FasL-mediated apoptosis [21, 22]. Signaling through TNFR2 drives MDSC survival by increasing cellular Fas-associated death domain-like IL-1 β -converting enzyme-inhibitory protein, which in turn, inhibits the activation of caspase

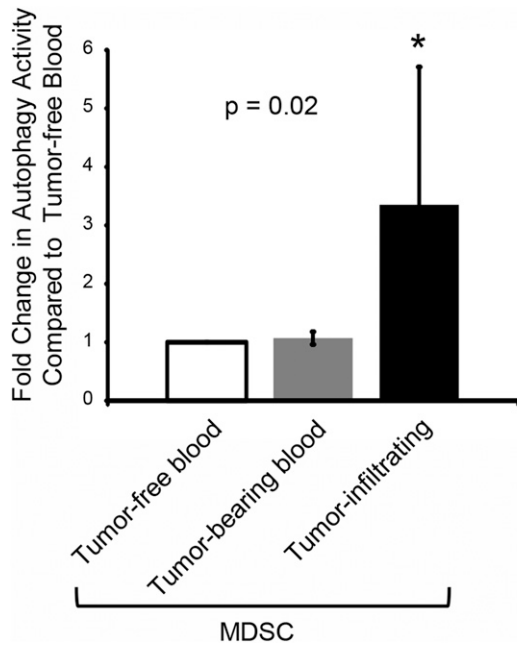


Figure 6. The TME promotes autophagy in MDSCs. Cells were obtained from the blood of tumor-free BALB/c mice or from the blood and tumors of 4T1 tumor-bearing (tumor-infiltrating) BALB/c mice. Cells were stained for CD45, Gr1, and CD11b along with Cyto-ID, and the gated CD45⁺Gr1⁺CD11b⁺ cells (MDSCs) were analyzed by flow cytometry for Cyto-ID expression. Data are the average fold change in autophagy activity compared with the naïve blood sample. * $P = 0.02$, statistical significant difference compared with tumor-free samples. Data are averaged from 7 mice in 3 independent experiments.

8, thereby disrupting apoptosis [23]. Activation through the IL-4R α (CD124), which is expressed on some MDSCs, has also been implicated in extending MDSC survival by inhibiting STAT6 phosphorylation and blocking MDSC apoptosis [24]. MDSC survival is also regulated by the transcription factor IRF8 [25, 26]. MDSCs down-regulate IRF8, which modulates expression of the antiapoptotic molecules Bcl-2-associated X protein and B cell lymphoma-extra large protein, thereby preventing apoptosis. Whether any of these effector molecules or transcription factors are regulated by HMGB1 or vice versa or whether HMGB1 identifies a distinct regulatory pathway remains to be determined.

Autophagy has not been examined previously as a mechanism for sustaining the survival of MDSCs, yet many of the conditions and effector molecules that are known to facilitate MDSC survival can be linked to autophagy. For example, hypoxia-inducible factor 1 α , an established inducer of autophagy [27], promotes MDSC survival by redirecting MDSCs in the TME toward a tumor-associated macrophage phenotype [28]. ROS, a family of effector molecules that regulate autophagy [29], also drive MDSC accumulation and survival. ROS mediate their effects by regulating the cellular stress sensor CHOP in MDSCs [30], and activation of CHOP has been linked to autophagy, in that CHOP promotes increased transcription of essential autophagy proteins Atg5 and LC3 [31]. Endoplasmic reticulum stress also induces autophagy [32, 33] and regulates MDSC half-life by controlling TRAIL receptor expression on MDSCs [34].

Therefore, autophagy may be a unifying mechanism by which many MDSC inducers increase MDSC quantity and half-life.

Many of the conditions that have the potential to induce autophagy are present in the TME and are linked to HMGB1, so it is not unexpected that HMGB1 regulates the survival of MDSCs by driving autophagy. For example, the TME of solid tumors is frequently an inflammatory environment, and inflammation promotes autophagy [35]. HMGB1 is one of the proinflammatory molecules that contributes to the inflammatory milieu, and HMGB1 drives the accumulation of MDSCs [10], which themselves, release ROS, which are common within solid tumors. ROS promote the extracellular release of HMGB1 [36], and HMGB1 release is enhanced by autophagy [13]. Given the prevalence of ROS and HMGB1 in the TME, it is likely that tumor-induced MDSCs are proautophagic as a result of exposure to these 2 molecules.

Conditions in the TME, including inflammation and hypoxia, promote autophagy [29, 37, 38] and MDSC-suppressive potency [9, 28, 39, 40]. As tumor-infiltrating MDSCs have heightened suppressor function relative to circulating MDSCs [18, 28], our finding that autophagy decreases MDSC function appears to be contradictory. This apparent inconsistency could be a result of other factors in the TME that drive MDSC potency and over-ride the effects of autophagy on MDSC function. Metabolism and the use of energy could possibly explain the increase in MDSC-suppressive potency when autophagy is blocked. Chloroquine and bafilomycin, the reagents used here to inhibit autophagy and increase MDSC-mediated suppression, block lysosomal acidification and autophagosome-lysosome fusion, thus limiting protein degradation [41]. Under these conditions the energy expended on protein degradation might be redirected and used to drive immune-suppressive functions. Alternatively, as autophagy increases MDSC half-life, tumor-infiltrating MDSCs may be more suppressive, as they mediate suppression over a longer period of time. The TME is obviously a complicated locale, so the net result for MDSC-suppressive potency depends on the interactions of multiple conditions.

The role of autophagy in promoting tumor progression is well established and has been attributed to its ability to increase the survival of tumor cells [3, 42]. The studies reported here demonstrate that autophagy also supports tumor progression by sustaining the survival of MDSCs. Therefore, autophagy not only enhances tumor progression as a result of a direct impact on tumor cells but also by facilitating tumor-induced immune suppression and inhibiting anti-tumor immunity.

AUTHORSHIP

K.H.P. and S.O.-R. designed experiments, analyzed data, and wrote the manuscript. K.H.P. and L.A.H. performed experiments. All authors approved the manuscript.

ACKNOWLEDGMENTS

This work was supported by grants from the U.S. National Institutes of Health (RO1 GM021248, RO1 CA115880, and RO1 CA84232). The authors thank Dr. Michael Lotze for helpful discussions.

DISCLOSURES

The authors declare no conflicts of interest.

REFERENCES

- Balkwill, F., Mantovani, A. (2001) Inflammation and cancer: back to Virchow? *Lancet* **357**, 539–545.
- White, E. (2012) Deconvoluting the context-dependent role for autophagy in cancer. *Nat. Rev. Cancer* **12**, 401–410.
- Yang, X., Yu, D. D., Yan, F., Jing, Y. Y., Han, Z. P., Sun, K., Liang, L., Hou, J., Wei, L. X. (2015) The role of autophagy induced by tumor microenvironment in different cells and stages of cancer. *Cell Biosci.* **5**, 14.
- Lum, J. J., Bauer, D. E., Kong, M., Harris, M. H., Li, C., Lindsten, T., Thompson, C. B. (2005) Growth factor regulation of autophagy and cell survival in the absence of apoptosis. *Cell* **120**, 237–248.
- Tang, D., Kang, R., Coyne, C. B., Zeh, H. J., Lotze, M. T. (2012) PAMPs and DAMPs: signal 0s that spur autophagy and immunity. *Immunol. Rev.* **249**, 158–175.
- Yorimitsu, T., Klionsky, D. J. (2005) Autophagy: molecular machinery for self-eating. *Cell Death Differ.* **12** (Suppl 2), 1542–1552.
- Quail, D. F., Joyce, J. A. (2013) Microenvironmental regulation of tumor progression and metastasis. *Nat. Med.* **19**, 1423–1437.
- Gabrilovich, D. I., Ostrand-Rosenberg, S., Bronte, V. (2012) Coordinated regulation of myeloid cells by tumours. *Nat. Rev. Immunol.* **12**, 253–268.
- Ostrand-Rosenberg, S., Sinha, P. (2009) Myeloid-derived suppressor cells: linking inflammation and cancer. *J. Immunol.* **182**, 4499–4506.
- Parker, K. H., Sinha, P., Horn, L. A., Clements, V. K., Yang, H., Li, J., Tracey, K. J., Ostrand-Rosenberg, S. (2014) HMGB1 enhances immune suppression by facilitating the differentiation and suppressive activity of myeloid-derived suppressor cells. *Cancer Res.* **74**, 5723–5733.
- Tang, D., Kang, R., Livesey, K. M., Cheh, C. W., Farkas, A., Loughran, P., Hoppe, G., Bianchi, M. E., Tracey, K. J., Zeh III, H. J., Lotze, M. T. (2010) Endogenous HMGB1 regulates autophagy. *J. Cell Biol.* **190**, 881–892.
- Sinha, P., Clements, V. K., Ostrand-Rosenberg, S. (2005) Reduction of myeloid-derived suppressor cells and induction of M1 macrophages facilitate the rejection of established metastatic disease. *J. Immunol.* **174**, 636–645.
- Tang, D., Kang, R., Cheh, C. W., Livesey, K. M., Liang, X., Schapiro, N. E., Benschop, R., Sparvero, L. J., Amoscatto, A. A., Tracey, K. J., Zeh, H. J., Lotze, M. T. (2010) HMGB1 release and redox regulates autophagy and apoptosis in cancer cells. *Oncogene* **29**, 5299–5310.
- Ulloa, L., Ochani, M., Yang, H., Tanovic, M., Halperin, D., Yang, R., Czura, C. J., Fink, M. P., Tracey, K. J. (2002) Ethyl pyruvate prevents lethality in mice with established lethal sepsis and systemic inflammation. *Proc. Natl. Acad. Sci. USA* **99**, 12351–12356.
- Guo, S., Liang, Y., Murphy, S. F., Huang, A., Shen, H., Kelly, D. F., Sobrado, P., Sheng, Z. (2015) A rapid and high content assay that measures cyto-ID-stained autophagic compartments and estimates autophagy flux with potential clinical applications. *Autophagy* **11**, 560–572.
- Oeste, C. L., Seco, E., Patton, W. F., Boya, P., Pérez-Sala, D. (2013) Interactions between autophagic and endo-lysosomal markers in endothelial cells. *Histochem. Cell Biol.* **139**, 659–670.
- Porter, K., Nallathambi, J., Lin, Y., Liton, P. B. (2013) Lysosomal basification and decreased autophagic flux in oxidatively stressed trabecular meshwork cells: implications for glaucoma pathogenesis. *Autophagy* **9**, 581–594.
- Sinha, P., Chornoguz, O., Clements, V. K., Artemenko, K. A., Zubarev, R. A., Ostrand-Rosenberg, S. (2011) Myeloid-derived suppressor cells express the death receptor Fas and apoptose in response to T cell-expressed FasL. *Blood* **117**, 5381–5390.
- Bunt, S. K., Yang, L., Sinha, P., Clements, V. K., Leips, J., Ostrand-Rosenberg, S. (2007) Reduced inflammation in the tumor microenvironment delays the accumulation of myeloid-derived suppressor cells and limits tumor progression. *Cancer Res.* **67**, 10019–10026.
- Bunt, S. K., Sinha, P., Clements, V. K., Leips, J., Ostrand-Rosenberg, S. (2006) Inflammation induces myeloid-derived suppressor cells that facilitate tumor progression. *J. Immunol.* **176**, 284–290.
- Chornoguz, O., Grmai, L., Sinha, P., Artemenko, K. A., Zubarev, R. A., Ostrand-Rosenberg, S. (2011) Proteomic pathway analysis reveals inflammation increases myeloid-derived suppressor cell resistance to apoptosis. *Mol. Cell. Proteomics* **10**, M110.002980.
- Ostrand-Rosenberg, S., Sinha, P., Chornoguz, O., Ecker, C. (2012) Regulating the suppressors: apoptosis and inflammation govern the survival of tumor-induced myeloid-derived suppressor cells (MDSC). *Cancer Immunol. Immunother.* **61**, 1319–1325.
- Zhao, X., Rong, L., Zhao, X., Li, X., Liu, X., Deng, J., Wu, H., Xu, X., Erben, U., Wu, P., Syrbe, U., Sieper, J., Qin, Z. (2012) TNF signaling drives myeloid-derived suppressor cell accumulation. *J. Clin. Invest.* **122**, 4094–4104.
- Roth, F., De La Fuente, A. C., Vella, J. L., Zoso, A., Inverardi, L., Serafini, P. (2012) Aptamer-mediated blockade of IL4Rα triggers apoptosis of MDSCs and limits tumor progression. *Cancer Res.* **72**, 1373–1383.
- Wright, J. D., Netherby, C., Hensen, M. L., Miller, A., Hu, Q., Liu, S., Bogner, P. N., Farren, M. R., Lee, K. P., Liu, K., Abrams, S. I. (2013) Myeloid-derived suppressor cell development is regulated by a STAT/IRF-8 axis. *J. Clin. Invest.* **123**, 4464–4478.
- Messmer, M. N., Netherby, C. S., Banik, D., Abrams, S. I. (2015) Tumor-induced myeloid dysfunction and its implications for cancer immunotherapy. *Cancer Immunol. Immunother.* **64**, 1–13.
- Bellot, G., Garcia-Medina, R., Gounon, P., Chiche, J., Roux, D., Pouyssegur, J., Mazure, N. M. (2009) Hypoxia-induced autophagy is mediated through hypoxia-inducible factor induction of BNIP3 and BNIP3L via their BH3 domains. *Mol. Cell. Biol.* **29**, 2570–2581.
- Corzo, C. A., Condamine, T., Lu, L., Cotter, M. J., Youn, J. I., Cheng, P., Cho, H. I., Celis, E., Quiceno, D. G., Padhya, T., McCaffrey, T. V., McCaffrey, J. C., Gabrilovich, D. I. (2010) HIF-1α regulates function and differentiation of myeloid-derived suppressor cells in the tumor microenvironment. *J. Exp. Med.* **207**, 2439–2453.
- Scherz-Shouval, R., Elazar, Z. (2011) Regulation of autophagy by ROS: physiology and pathology. *Trends Biochem. Sci.* **36**, 30–38.
- Thevenot, P. T., Sierra, R. A., Raber, P. L., Al-Khami, A. A., Trillo-Tinoco, J., Zarreii, P., Ochoa, A. C., Cui, Y., Del Valle, L., Rodriguez, P. C. (2014) The stress-response sensor chop regulates the function and accumulation of myeloid-derived suppressor cells in tumors. *Immunity* **41**, 389–401.
- Rouschop, K. M., van den Beucken, T., Dubois, L., Niessen, H., Bussink, J., Savelkoul, K., Keulers, T., Mujic, H., Landuyt, W., Voncken, J. W., Lambin, P., van der Kogel, A. J., Koritzinsky, M., Wouters, B. G. (2010) The unfolded protein response protects human tumor cells during hypoxia through regulation of the autophagy genes MAP1LC3B and ATG5. *J. Clin. Invest.* **120**, 127–141.
- Ogata, M., Hino, S., Saito, A., Morikawa, K., Kondo, S., Kanemoto, S., Murakami, T., Taniguchi, M., Tani, I., Yoshinaga, K., Shiosaka, S., Hammarback, J. A., Urano, F., Imaizumi, K. (2006) Autophagy is activated for cell survival after endoplasmic reticulum stress. *Mol. Cell. Biol.* **26**, 9220–9231.
- Yorimitsu, T., Nair, U., Yang, Z., Klionsky, D. J. (2006) Endoplasmic reticulum stress triggers autophagy. *J. Biol. Chem.* **281**, 30299–30304.
- Condamine, T., Kumar, V., Ramachandran, I. R., Youn, J. I., Celis, E., Finnberg, N., El-Deiry, W. S., Winograd, R., Vonderheide, R. H., English, N. R., Knight, S. C., Yagita, H., McCaffrey, J. C., Antonia, S., Hockstein, N., Witt, R., Masters, G., Bauer, T., Gabrilovich, D. I. (2014) ER stress regulates myeloid-derived suppressor cell fate through TRAIL-R-mediated apoptosis. *J. Clin. Invest.* **124**, 2626–2639.
- Mathew, R., Karantzis-Wadsworth, V., White, E. (2007) Role of autophagy in cancer. *Nat. Rev. Cancer* **7**, 961–967.
- Tang, D., Kang, R., Livesey, K. M., Zeh III, H. J., Lotze, M. T. (2011) High mobility group box 1 (HMGB1) activates an autophagic response to oxidative stress. *Antioxid. Redox Signal.* **15**, 2185–2195.
- Joven, J., Guirro, M., Mariné-Casado, R., Rodríguez-Gallego, E., Menéndez, J. A. (2014) Autophagy is an inflammation-related defensive mechanism against disease. *Adv. Exp. Med. Biol.* **824**, 43–59.
- Martinez-Outschoorn, U. E., Trimmer, C., Lin, Z., Whitaker-Menezes, D., Chiavarina, B., Zhou, J., Wang, C., Pavlides, S., Martinez-Cantarín, M. P., Capozza, F., Witkiewicz, A. K., Flomenberg, N., Howell, A., Pestell, R. G., Caro, J., Lisanti, M. P., Sotgia, F. (2010) Autophagy in cancer associated fibroblasts promotes tumor cell survival: role of hypoxia, HIF1 induction and NFκB activation in the tumor stromal microenvironment. *Cell Cycle* **9**, 3515–3533.
- Lu, T., Gabrilovich, D. I. (2012) Molecular pathways: tumor-infiltrating myeloid cells and reactive oxygen species in regulation of tumor microenvironment. *Clin. Cancer Res.* **18**, 4877–4882.
- Lu, T., Ramakrishnan, R., Altio, S., Youn, J. I., Cheng, P., Celis, E., Pisarev, V., Sherman, S., Sporn, M. B., Gabrilovich, D. (2011) Tumor-infiltrating myeloid cells induce tumor cell resistance to cytotoxic T cells in mice. *J. Clin. Invest.* **121**, 4015–4029.
- Tanida, I., Minematsu-Ikeguchi, N., Ueno, T., Kominami, E. (2005) Lysosomal turnover, but not a cellular level, of endogenous LC3 is a marker for autophagy. *Autophagy* **1**, 84–91.
- Fung, C., Lock, R., Gao, S., Salas, E., Debnath, J. (2008) Induction of autophagy during extracellular matrix detachment promotes cell survival. *Mol. Biol. Cell* **19**, 797–806.

KEY WORDS:

tumor-induced immune suppression · tumor microenvironment · DAMPs